Available online at www.sciencedirect.com
ScienceDirect
International Journal of Heat and Mass Transfer 51 (2008) 4300–4314
International Journal of HEAT and MASS TRANSFER
www.elsevier.com/locate/ijhmt

Extensive study on laminar free film condensation from vapor–gas mixture

De-Yi Shang [a,*], Liang-Cai Zhong [b]

[a] 286 Woodfield Dr. Ottawa, ON, Canada K2G 3W9
[b] Northeastern University, Shenyang 110004, PR China

Received 18 June 2007; received in revised form 28 February 2008
Available online 24 May 2008

Abstract

The dimensionless velocity component method was successfully applied in a depth investigation of laminar free film condensation from a vapor–gas mixture, and the complete similarity transformation of its system of governing partial differential equations was conducted. The set of dimensionless variables of the transformed mathematical model greatly facilitates the analysis and calculation of the velocity, temperature and concentration fields, and heat and mass transfer of the film condensation from the vapor–gas mixture. Meanwhile, three difficult points of analysis related to the reliable analysis and calculation of heat and mass transfer for the film condensation from the vapor–gas mixture were overcome. They include: (i) correct determination of the interfacial vapor condensate saturated temperature; (ii) reliable treatment of the concentration-dependent densities of vapor–gas mixture, and (iii) rigorously satisfying the whole set of physical matching conditions at the liquid–vapor interface. Furthermore, the critical bulk vapor mass fraction for condensation was proposed, and evaluated for the film condensation from the water vapor–air mixture, and the useful methods in treatment of temperature-dependent physical properties of liquids and gases were applied. With these elements in place, the reliable results on analysis and calculation of heat and mass transfer of the film condensation from the vapor–gas mixture were achieved.

The laminar free film condensation of water vapor in the presence of air was taken as an example for the numerical calculation. It was confirmed that the presence of the non-condensable gas is a decisive factor in decreasing the heat and mass transfer of the film condensation. It was demonstrated that an increase of the bulk gas mass fraction has the following impacts: an expedited decline in the interfacial vapor condensate saturation temperature; an expedited decrease in the condensate liquid film thickness, the condensate liquid velocity, and the condensate heat and mass transfer. It was found that an increase of the wall temperature will increase the negative effect of the non-condensable gas on heat and mass transfer of the film condensation from the vapor–gas mixture.

1. Introduction

Vapor film condensation plays an important role in many industrial applications, especially, the chemical and power industries, including nuclear power plants. To date, numerous efforts have investigated its physical phenomena; some detailed reviews of condensation heat and mass transfer can be found in Refs. [1–5]. Meanwhile, film condensation from vapor in presence of non-condensable gas is even practical area in the design of heat exchangers. In its investigation, Minkowycz and Sparrow [6] presented their investigation of laminar free film condensation of steam in the presence of non-condensable gas. Numerous theoretical and experimental studies have followed, and only some of them, such as in Refs. [7–20] are listed here due to the space limitation. These studies demonstrated that the bulk concentration of the non-condensable gas could have a great reduction in heat transfer. This is due to the fact that the presence of non-condensable gas lowers the partial pressure of the vapor, and then reduces the interfacial vapor condensate saturation temperature.

However, based on the authors' research, there remain three difficult points that need to be addressed to ensure correct analysis and calculation of heat and mass transfer of the film condensation from the vapor–gas mixture.

* Corresponding author.
E-mail address: deyishang@yahoo.ca (D.-Y. Shang).

0017-9310/$ - see front matter © 2008 Elsevier Ltd. All rights reserved.
doi:10.1016/j.ijheatmasstransfer.2008.03.004

Nomenclature

$C_{m,g}$	gas mass fraction
$C^*_{m,g\infty}$	critical bulk gas mass fraction with $t_s - t_w = 0$
$C_{m,v}$	vapor mass fraction
c_p	specific heat, J/(kg °C)
D_v	vapor mass diffusion coefficient in gas, m^2/s
g	gravitation acceleration, m/s^2
g_x	local mass flow rate entering the liquid film at position x related to per unit area of the plate, kg/m^2 s
G_x	total mass flow rate entering the liquid film for position $x = 0$ to x with width b of the plate, kg/s
$Gr_{xl,s}$	local Grashof number of condensate liquid film
$Gr_{xv,\infty}$	local Grashof number of vapor–gas mixture film
$Nu_{xl,w}$	local Nusselt number
$n_{\lambda,g}$	thermal conductivity parameter of gas
$n_{\lambda,v}$	thermal conductivity parameter of vapor
$n_{\mu,g}$	viscosity parameter of gas
$n_{\mu,v}$	viscosity parameter of vapor
Pr	Prandtl number
q_x	local heat transfer rate at position x per unit area on the plate, W/m^2
Q_x	total heat transfer rate for $x = 0$ to x with width of b on the plate, W
$Sc_{m,\infty}$	local Schmidt number
t	temperature, °C
T	absolute temperature, K
T_w	wall temperature, K
T_s	vapor saturated temperature at the liquid–vapor interface, K
T_∞	bulk temperature, K
w_{xl}, w_{yl}	condensate liquid velocity components in x- and y-coordinates, respectively, m/s
w_{xv}, w_{yv}	vapor–gas mixture velocity components in x and y-coordinates, respectively, m/s
W_{xl}, $W_{xl,}$	dimensionless condensate liquid velocity components in x- and y-coordinates, respectively
W_{xv}, W_{yv}	dimensionless vapor–gas mixture velocity components in x- and y-coordinates, respectively

Greek symbols

δ_c	concentration boundary layer thickness of vapor–gas mixture, m
δ_l	condensate liquid film thickness, m
δ_v	momentum boundary layer thickness of vapor–gas mixture, m
η_l	dimensionless co-ordinate variable of condensate liquid film
η_v	dimensionless co-ordinate variable of vapor–gas mixture film
ρ_g	gas density, kg/m^3
ρ_v	vapor density, kg/m^3
$\rho_{m,g}$	local density of gas in vapor–gas mixture
$\rho_{m,v}$	local density of vapor in vapor–gas mixture
ρ_m	density of vapor–gas mixture
μ	absolute viscosity, kg/m s
λ	thermal conductivity, W/(m K)
v	kinetic viscosity, m^2/s
θ_l	dimensionless temperature of condensate liquid film
θ_v	dimensionless temperature of vapor–gas mixture film
$\Gamma_{m,v}$	vapor relative mass fraction
α_x	local heat transfer coefficient, $W/(m^2 K)$
Φ_s	condensate mass flow rate parameter

Subscripts

c	concentration
g	gas
l	liquid
m	vapor–gas mixture
s	saturated state or state at liquid–vapor interface
v	vapor
∞	in the bulk

These points include, (i) correct determination of the interfacial vapor saturated temperature, (ii) rigorous treatment of the concentration-dependent densities of vapor–gas mixture, and (iii) rigorously satisfying the whole set of physical matching conditions at the liquid–vapor interface. The purpose of this study is to develop a complete system of mathematical models for overcoming these areas of uncertainty.

2. Governing equations

2.1. Governing partial differential equations

The analytical model and coordinate system used for laminar free film condensation of vapor with non-condensable gas on an isothermal vertical flat plate is shown in Fig. 1. An isothermal vertical flat plate is suspended in a large volume of quiescent vapor–gas mixture at atmospheric pressure. The plate temperature is T_w, the temperature of the vapor–gas mixture bulk is T_∞, and the vapor condensate saturated temperature dependent on its partial pressure is T_s. If given condition for the model is $T_w < T_s$, a steady film condensation will occur on the plate. We assume that the laminar flow within the liquid film is induced by gravity, and the vapor–gas mixture film flow is caused by the shear force at the liquid–vapor interface. We further assume that the mass flow rate of vapor is balanced to the vapor mass diffusion at the liquid–vapor interface in the steady state of the laminar free film

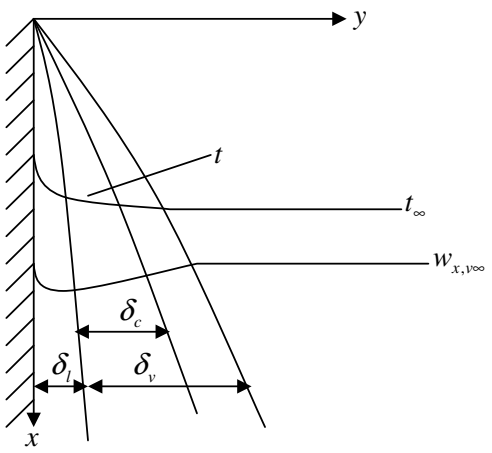

Fig. 1. Physical model and coordinate system of the film condensation from vapor–gas mixture.

condensation. Under these conditions, there is never an additional gas boundary layer near the interface except the induced concentration boundary layer of the vapor–gas mixture. In addition, we take into account the temperature-dependent physical properties of the condensate liquid film, and the temperature- and concentration-dependent physical properties of the induced vapor–gas mixture film. Then, the steady laminar governing partial differential equations for mass, momentum, energy and concentration conservations in the two-phase boundary layer are as follows:

The governing partial differential equations for condensate liquid film are

$$\frac{\partial}{\partial x}(\rho_l w_{xl}) + \frac{\partial}{\partial y}(\rho_l w_{yl}) = 0 \tag{1}$$

$$\rho_l\left(w_{xl}\frac{\partial w_{xl}}{\partial x} + w_{yl}\frac{\partial w_{xl}}{\partial y}\right) = \frac{\partial}{\partial y}\left(\mu_l\frac{\partial w_{xl}}{\partial y}\right) + g(\rho_l - \rho_{m,\infty}) \tag{2}$$

$$\rho_l c_{pl}\left(w_{xl}\frac{\partial T_l}{\partial x} + w_{yl}\frac{\partial T_l}{\partial y}\right) = \frac{\partial}{\partial y}\left(\lambda_l\frac{\partial T_l}{\partial y}\right) \tag{3}$$

where Eqs. (1)–(3) are continuity, momentum and energy conservation equations, respectively.

The governing partial differential equations for vapor–gas mixture film are

$$\frac{\partial}{\partial x}(\rho_m w_{xv}) + \frac{\partial}{\partial y}(\rho_m w_{yv}) = 0 \tag{4}$$

$$\rho_m\left(w_{xv}\frac{\partial w_{xv}}{\partial x} + w_{yv}\frac{\partial w_{xv}}{\partial y}\right) = \frac{\partial}{\partial y}\left(\mu_m\frac{\partial w_{xv}}{\partial y}\right) + g(\rho_m - \rho_{m,\infty}) \tag{5}$$

$$\rho_m c_{p_m}\left(w_{xv}\frac{\partial T_v}{\partial x} + w_{yv}\frac{\partial T_v}{\partial y}\right) = \frac{\partial}{\partial y}\left(\lambda_m\frac{\partial T_v}{\partial y}\right) + \frac{\partial}{\partial y}\left[\rho_m D_v(c_{p_v} - c_{p_g})\frac{\partial C_{m,v}}{\partial y}t_v\right] \tag{6}$$

$$\frac{\partial(w_{xv}\rho_m C_{m,v})}{\partial x} + \frac{\partial(w_{yv}\rho_m C_{m,v})}{\partial y} = \frac{\partial}{\partial y}\left(D_v\rho_m\frac{\partial C_{m,v}}{\partial y}\right) \tag{7}$$

where Eqs. (4)–(6) are continuity, momentum, and energy conservation equations. Eq. (7) is the species conservation equation with mass diffusion. Here, $C_{m,v}$ is vapor mass fraction, ρ_m, μ_m, λ_m and Cp_m are density, absolute viscosity, thermal conductivity and specific heat of the vapor–gas mixture, respectively, and D_v denotes the vapor mass diffusion coefficient in the non-condensable gas.

The boundary conditions are

$$y = 0: \quad w_{xl} = 0,\ w_{yl} = 0,\ T_l = T_w \tag{8}$$

$y = \delta_l$:

$$w_{xl,s} = w_{xv,s} \tag{9}$$

$$\rho_{l,s}\left(w_{xl}\frac{\partial\delta_l}{\partial x} - w_{yl}\right)_{l,s} = \rho_{m,s}C_{m,vs}\left(w_{xv}\frac{\partial\delta_v}{\partial x} - w_{yv}\right)_{v,s} = g_x \tag{10}$$

$$\mu_{l,s}\left(\frac{\partial w_{xl}}{\partial y}\right)_s = \mu_{m,s}\left(\frac{\partial w_{xv}}{\partial y}\right)_s \tag{11}$$

$$\lambda_{l,s}\left(\frac{\partial T_l}{\partial y}\right)_{y=\delta_l} = \lambda_{m,s}\left(\frac{\partial T_v}{\partial y}\right)_{y=\delta_l} + h_{fg}\rho_{m,s}C_{m,vs}\left(w_{xv}\frac{\partial\delta_v}{\partial x} - w_{yv}\right)_s \tag{12}$$

$$T = T_s \tag{13}$$

$$C_{m,v} = C_{m,vs} \tag{14}$$

$$\rho_{m,s}C_{m,vs}\left(w_{xv}\frac{\partial\delta}{\partial x} - w_{yv}\right)_{v,s} = D_v\rho_{m,s}\left(\frac{\partial C_{m,v}}{\partial y}\right)_s \tag{15}$$

$y \to \infty$:

$$w_{xv} \to 0, \quad T_v = T_\infty, \quad C_{m,v} = C_{m,v\infty} \tag{16}$$

where Eq. (8) expresses the physical conditions on the plate. Eqs. (9)–(15) express the physical matching conditions at the liquid–vapor interface. Eq. (9) expresses the velocity component continuity, Eq. (10) expresses the mass flow rate continuity, Eq. (11) expresses the balance of the shear force, Eq. (12) expresses the energy balance, Eq. (13) expresses the temperature continuity, Eq. (14) expresses the related concentration condition, and Eq. (15) expresses the vapor mass flow rate is balanced to the mass flow rate caused by the vapor mass diffusion, Eq. (16) expresses the physical conditions in the vapor–gas mixture bulk. In addition, $C_{m,vs}$ and $C_{m,v\infty}$ denote the vapor mass fraction at the interface and bulk, respectively.

It is necessary to explain Eq. (15) for the condition of interfacial mass diffusion balance. Originally, it should be

$$\left[\rho_l\left(w_x\frac{\partial\delta_l}{\partial x} - w_y\right)\right]_{l,s} = \left[\rho_{m,s}C_{m,v}\left(w_x\frac{\partial\delta}{\partial x} - w_y\right)\right]_{v,s} \equiv \rho_{m,s}D_v\left(\frac{\partial C_{m,v}}{\partial y}\right) \tag{15 orig.}$$

In order to conveniently transform the balance condition equation to the dimensionless form, we take Eq. (15) to express the interfacial mass diffusion balance condition. This form of expression has never caused any change of the calculation results.

2.2. Similarity transformation

Applying the dimensionless velocity component method [5], we assume the following dimensionless variables for similarity transformation of the governing partial differential equations of the laminar free film condensation from the vapor–gas mixture.

For liquid film, the dimensionless variables are assumes as

$$\eta_{\mathrm{l}} = \left(\frac{1}{4}Gr_{x\mathrm{l,s}}\right)^{1/4}\frac{y}{x} \tag{17}$$

$$Gr_{x\mathrm{l,s}} = \frac{g(\rho_{\mathrm{l,w}}-\rho_{\mathrm{m},\infty})x^3}{\nu_{\mathrm{l,s}}^2\rho_{\mathrm{l,s}}} \tag{18}$$

$$\theta_{\mathrm{l}} = \frac{T-T_{\mathrm{s}}}{T_{\mathrm{w}}-T_{\mathrm{s}}} \tag{19}$$

$$W_{x\mathrm{l}} = \left(2\sqrt{gx}\left(\frac{\rho_{\mathrm{l,w}}-\rho_{\mathrm{m},\infty}}{\rho_{\mathrm{l,s}}}\right)^{1/2}\right)^{-1} w_{x\mathrm{l}} \tag{20}$$

$$W_{y\mathrm{l}} = \left(2\sqrt{gx}\left(\frac{\rho_{\mathrm{l,w}}-\rho_{\mathrm{m},\infty}}{\rho_{\mathrm{l,s}}}\right)^{1/2}\left(\frac{1}{4}Gr_{x\mathrm{l,s}}\right)^{-4}\right)^{-1} w_{y\mathrm{l}} \tag{21}$$

where η_{l} is the dimensionless coordinate variable, $Gr_{x\mathrm{l,s}}$ is the local Grashof number, θ_{l} is the dimensionless temperature, and $W_{x\mathrm{l}}$ and $W_{y\mathrm{l}}$ are the dimensionless velocity components in x- and y-coordinates of the condensate liquid film, respectively. Here, $\rho_{\mathrm{l,w}}$ is the condensate liquid density on the wall, $\nu_{\mathrm{l,s}}$ and $\rho_{\mathrm{l,s}}$ are condensate liquid kinetic viscosity and density at the liquid–vapor interface, while, $\rho_{\mathrm{m},\infty}$ is density of vapor–gas mixture bulk.

For vapor–gas mixture film, the dimensionless variables are assumes as

$$\eta_{\mathrm{v}} = \left(\frac{1}{4}Gr_{x\mathrm{v},\infty}\right)^{1/4}\frac{y}{x} \tag{22}$$

$$Gr_{x\mathrm{v},\infty} = \frac{g(\rho_{\mathrm{m,s}}/\rho_{\mathrm{m},\infty}-1)x^3}{\nu_{\mathrm{m},\infty}^2} \tag{23}$$

$$\theta_{\mathrm{v}} = \frac{T-T_{\infty}}{T_{\mathrm{s}}-T_{\infty}} \tag{24}$$

$$W_{x\mathrm{v}} = \left(2\sqrt{gx}(\rho_{\mathrm{m,s}}/\rho_{\mathrm{m},\infty}-1)^{1/2}\right)^{-1} w_{x\mathrm{v}} \tag{25}$$

$$W_{y\mathrm{v}} = \left(2\sqrt{gx}(\rho_{\mathrm{m,s}}/\rho_{\mathrm{m},\infty}-1)^{1/2}\left(\frac{1}{4}Gr_{x\mathrm{v},\infty}\right)^{-1/4}\right)^{-1} w_{y\mathrm{v}} \tag{26}$$

$$\Gamma_{\mathrm{m,v}} = \frac{C_{\mathrm{m,v}}-C_{\mathrm{m,v}\infty}}{C_{\mathrm{m,vs}}-C_{\mathrm{m,v}\infty}} \tag{27}$$

where η_{v} is the *dimensionless coordinate variables*, $Gr_{x\mathrm{v},\infty}$ is the *local Grashof number*, θ_{v} is the dimensionless temperature, $W_{x\mathrm{v}}$ and $W_{y\mathrm{v}}$ are the dimensionless velocity components in x- and y-coordinates, and $\Gamma_{\mathrm{m,v}}$ is the vapor relative mass fraction of the vapor–gas mixture film, respectively. Here, $\rho_{\mathrm{m,s}}$ is interfacial density of vapor–gas mixture.

2.3. Governing ordinary differential equations

For liquid film

With the assumed transformation variables for the liquid film shown in Eqs. (17)–(21), the governing partial differential Eqs. (1)–(3) of the liquid film are equivalently transformed to the following dimensionless ordinary ones, respectively:

$$2W_{x\mathrm{l}} - \eta_{\mathrm{l}}\frac{\mathrm{d}W_{x\mathrm{l}}}{\mathrm{d}\eta_{\mathrm{l}}} + 4\frac{\mathrm{d}W_{y\mathrm{l}}}{\mathrm{d}\eta_{\mathrm{l}}} - \frac{1}{\rho_{\mathrm{l}}}\frac{\mathrm{d}\rho_{\mathrm{l}}}{\mathrm{d}\eta_{\mathrm{l}}}[\eta_{\mathrm{l}}W_{x\mathrm{l}} - 4W_{y\mathrm{l}}] = 0 \tag{28}$$

$$\frac{\nu_{\mathrm{l,s}}}{\nu_{\mathrm{l}}}\left[W_{x\mathrm{l}}\left(2W_{x\mathrm{l}} - \eta_{\mathrm{l}}\frac{\mathrm{d}W_{x\mathrm{l}}}{\mathrm{d}\eta_{\mathrm{l}}}\right) + 4W_{y\mathrm{l}}\frac{\mathrm{d}W_{x\mathrm{l}}}{\mathrm{d}\eta_{\mathrm{l}}}\right] = \frac{\mathrm{d}^2W_{x\mathrm{l}}}{\mathrm{d}\eta_{\mathrm{l}}^2} + \frac{1}{\mu_{\mathrm{l}}}\frac{\mathrm{d}\mu_{\mathrm{l}}}{\mathrm{d}\eta_{\mathrm{l}}}\frac{\mathrm{d}W_{x\mathrm{l}}}{\mathrm{d}\eta_{\mathrm{l}}} + \frac{\mu_{\mathrm{l,s}}}{\mu_{\mathrm{l}}}\frac{\rho_{\mathrm{l}}-\rho_{\mathrm{m},\infty}}{\rho_{\mathrm{l,w}}-\rho_{\mathrm{m},\infty}} \tag{29}$$

$$\frac{\nu_{\mathrm{l,s}}}{\nu_{\mathrm{l}}}(-\eta_{\mathrm{l}}W_{x\mathrm{l}} + 4W_{y\mathrm{l}})\frac{\mathrm{d}\theta_{\mathrm{l}}}{\mathrm{d}\eta_{\mathrm{l}}} = \frac{1}{Pr_{\mathrm{l}}}\left(\frac{\mathrm{d}^2\theta_{\mathrm{l}}}{\mathrm{d}\eta_{\mathrm{l}}^2} + \frac{1}{\lambda_{\mathrm{l}}}\frac{\mathrm{d}\lambda_{\mathrm{l}}}{\mathrm{d}\eta_{\mathrm{l}}}\frac{\mathrm{d}\theta_{\mathrm{l}}}{\mathrm{d}\eta_{\mathrm{l}}}\right) \tag{30}$$

For vapor–gas mixture film

With the assumed similarity transformation variables for vapor–gas mixture film shown in Eqs. (22)–(27), the governing partial differential Eqs. (4)–(7) are transformed equivalently to the following dimensionless ones, respectively:

$$2W_{x\mathrm{v}} - \eta_{\mathrm{v}}\frac{\mathrm{d}W_{x\mathrm{v}}}{\mathrm{d}\eta} + 4\frac{\mathrm{d}W_{y\mathrm{v}}}{\mathrm{d}\eta_{\mathrm{v}}} - \frac{1}{\rho_{\mathrm{m}}}\frac{\mathrm{d}\rho_{\mathrm{m}}}{\mathrm{d}\eta_{\mathrm{v}}}(\eta_{\mathrm{v}}W_{x\mathrm{v}} - 4W_{y\mathrm{v}}) = 0 \tag{31}$$

$$\frac{\nu_{\mathrm{m},\infty}}{\nu_{\mathrm{m}}}\left[W_{x\mathrm{v}}\left(2W_{x\mathrm{v}} - \eta_{\mathrm{v}}\frac{\mathrm{d}W_{x\mathrm{v}}}{\mathrm{d}\eta}\right) + 4W_{y\mathrm{v}}\frac{\mathrm{d}W_{x\mathrm{v}}}{\mathrm{d}\eta_{\mathrm{v}}}\right] = \frac{\mathrm{d}^2W_{x\mathrm{v}}}{\mathrm{d}\eta_{\mathrm{v}}^2} + \frac{1}{\mu_{\mathrm{m}}}\frac{\mathrm{d}\mu_{\mathrm{m}}}{\mathrm{d}\eta_{\mathrm{v}}}\frac{\mathrm{d}W_{x\mathrm{v}}}{\mathrm{d}\eta_{\mathrm{v}}} + \frac{\mu_{\mathrm{m},\infty}}{\mu_{\mathrm{m}}}\frac{\rho_{\mathrm{m}}-\rho_{\mathrm{m},\infty}}{\rho_{\mathrm{m,s}}-\rho_{\mathrm{m},\infty}} \tag{32}$$

$$\begin{aligned}\frac{\nu_{\mathrm{m},\infty}}{\nu_{\mathrm{v,m}}}(-\eta_{\mathrm{v}}W_{x\mathrm{v}} + 4W_{y\mathrm{v}})\frac{\mathrm{d}\theta_{\mathrm{v}}}{\mathrm{d}\eta_{\mathrm{l}}} &= \frac{1}{Pr_{\mathrm{m}}}\left(\frac{\mathrm{d}^2\theta_{\mathrm{v}}}{\mathrm{d}\eta_{\mathrm{v}}^2} + \frac{1}{\lambda_{\mathrm{m}}}\frac{\mathrm{d}\lambda_{\mathrm{m}}}{\mathrm{d}\eta_{\mathrm{v}}}\frac{\mathrm{d}\theta_{\mathrm{v}}}{\mathrm{d}\eta_{\mathrm{v}}}\right) \\ &+ \frac{1}{Sc_{\mathrm{m},\infty}}\frac{\nu_{\mathrm{m},\infty}}{\nu_{\mathrm{m}}}(C_{\mathrm{m,vs}}-C_{\mathrm{m,v}\infty})\frac{c_{p_{\mathrm{v}}}-c_{p_{\mathrm{g}}}}{c_{p_{\mathrm{m}}}}\left[\frac{\mathrm{d}\Gamma_{\mathrm{m,v}}}{\mathrm{d}\eta_{\mathrm{v}}}\frac{\mathrm{d}\theta_{\mathrm{v}}}{\mathrm{d}\eta_{\mathrm{v}}}\right. \\ &\left. + \left(\theta_{\mathrm{v}} + \frac{T_{\infty}-273}{T_{\mathrm{s}}-T_{\infty}}\right)\frac{\mathrm{d}^2\Gamma_{\mathrm{m,v}}}{\mathrm{d}\eta_{\mathrm{v}}^2} + \left(\theta_{\mathrm{v}} + \frac{T_{\infty}-273}{T_{\mathrm{s}}-T_{\infty}}\right)\frac{1}{\rho_{\mathrm{m}}}\frac{\mathrm{d}\rho_{\mathrm{m}}}{\mathrm{d}\eta_{\mathrm{v}}}\frac{\mathrm{d}\Gamma_{\mathrm{m,v}}}{\mathrm{d}\eta_{\mathrm{v}}}\right]\end{aligned} \tag{33}$$

$$(-\eta_{\mathrm{v}}W_{x\mathrm{v}} + 4W_{y\mathrm{v}})\frac{\mathrm{d}\Gamma_{\mathrm{m,v}}}{\mathrm{d}\eta_{\mathrm{v}}} = \frac{1}{Sc_{\mathrm{m},\infty}}\left(\frac{\mathrm{d}^2\Gamma_{\mathrm{m,v}}}{\mathrm{d}\eta_{\mathrm{v}}^2} + \frac{1}{\rho_{\mathrm{m}}}\frac{\mathrm{d}\rho_{\mathrm{m}}}{\mathrm{d}\eta_{\mathrm{v}}}\frac{\mathrm{d}\Gamma_{\mathrm{m,v}}}{\mathrm{d}\eta_{\mathrm{v}}}\right) \tag{34}$$

where $Sc_{\mathrm{m},\infty} = \frac{\nu_{\mathrm{m},\infty}}{D_{\mathrm{v}}}$ is local Schmidt number, and Pr_{m} is Prandtl number of vapor–gas mixture.

For boundary conditions

With the corresponding transformation variables, the physical boundary conditions, Eqs. (8)–(16) are transformed equivalently to the following ones, respectively:

$$\eta_{\mathrm{l}}=0: \quad W_{x\mathrm{l}}=0,\ W_{y\mathrm{l}}=0,\ \theta_{\mathrm{l}}=1 \tag{35}$$

$$\eta_{\mathrm{l}}=\eta_{\mathrm{l}\delta}(\eta_{\mathrm{v}}=0):$$

$$W_{xv,\mathrm{s}}=\left(\frac{\rho_{\mathrm{l,w}}-\rho_{\mathrm{m},\infty}}{\rho_{\mathrm{l,s}}}\right)^{1/2}(\rho_{\mathrm{v,ms}}/\rho_{\mathrm{m},\infty}-1)^{-1/2}W_{x\mathrm{l,s}} \tag{36}$$

$$W_{yv,s}=-\frac{1}{4C_{\mathrm{m,vs}}}\frac{\rho_{\mathrm{l,s}}}{\rho_{\mathrm{m,s}}}\left(\frac{\nu_{\mathrm{l,s}}}{\nu_{\mathrm{m},\infty}}\right)^{1/2}\left(\frac{\rho_{\mathrm{l,w}}-\rho_{\mathrm{m},\infty}}{\rho_{\mathrm{l,s}}}\right)^{1/4}(\rho_{\mathrm{m,s}}/\rho_{\mathrm{m},\infty}-1)^{-1/4}(\eta_{\mathrm{l}\delta}W_{x\mathrm{l,s}}-4W_{y\mathrm{l,s}}) \tag{37}$$

$$\left(\frac{\mathrm{d}W_{xv}}{\mathrm{d}\eta_{\mathrm{v}}}\right)_{\mathrm{s}}=\frac{\mu_{\mathrm{l,s}}}{\mu_{\mathrm{m,s}}}\left(\frac{\nu_{\mathrm{m},\infty}}{\nu_{\mathrm{l,s}}}\right)^{1/2}\left(\frac{\rho_{\mathrm{l,w}}-\rho_{\mathrm{m},\infty}}{\rho_{\mathrm{l,s}}}\right)^{3/4}(\rho_{\mathrm{m,s}}/\rho_{\mathrm{m},\infty}-1)^{-3/4}\left(\frac{\mathrm{d}W_{x\mathrm{l}}}{\mathrm{d}\eta_{\mathrm{l}}}\right)_{\mathrm{s}} \tag{38}$$

$$\left(\frac{\mathrm{d}\theta_{\mathrm{v}}}{\mathrm{d}\eta_{\mathrm{v}}}\right)_{\mathrm{s}}=\frac{\lambda_{\mathrm{l,s}}(t_{\mathrm{w}}-t_{\mathrm{s}})\left(\frac{\mathrm{d}\theta_{\mathrm{l}}}{\mathrm{d}\eta_{\mathrm{l}}}\right)_{\mathrm{s}}\left(\frac{\nu_{\mathrm{m},\infty}}{\nu_{\mathrm{l,s}}}\right)^{1/2}\left(\frac{\rho_{\mathrm{l,w}}-\rho_{\mathrm{m},\infty}}{\rho_{\mathrm{l,s}}}\right)^{1/4}(\rho_{\mathrm{m,s}}/\rho_{\mathrm{m},\infty}-1)^{-1/4}-h_{\mathrm{fg}}C_{\mathrm{m,vs}}\rho_{\mathrm{m,s}}\nu_{\mathrm{m},\infty}(W_{xv,\mathrm{s}}\eta_{v\delta}-4W_{yv,s})}{\lambda_{\mathrm{m,s}}(T_{\mathrm{s}}-T_{\infty})} \tag{39}$$

$$\theta_{\mathrm{l}}=0, \quad \theta_{\mathrm{v}}=1, \tag{40}$$

$$\Gamma_{\mathrm{m,vs}}=1 \tag{41}$$

$$\left(\frac{\mathrm{d}\Gamma_{\mathrm{m,v}}}{\mathrm{d}\eta_{\mathrm{v}}}\right)_{\mathrm{s}}=-4Sc_{\mathrm{m},\infty}\frac{C_{\mathrm{m,vs}}}{(C_{\mathrm{m,vs}}-C_{\mathrm{m,v}\infty})}W_{yv,s} \tag{42}$$

$$\eta_{\mathrm{v}}\to\infty: \quad W_{xv}\to 0,\ \theta_{\mathrm{v}}\to 0,\ \Gamma_{\mathrm{m,v}\infty}=0 \tag{43}$$

The above transformation procedures are omitted here to save space.

The transformed governing Eqs. (28)–(34) are completely dimensionless because of the followings: (i) Eqs. (28)–(34) involve dimensionless velocity components $W_{x\mathrm{l}}$, $W_{y\mathrm{l}}$,W_{xv} and W_{yv}, dimensionless temperatures θ_{l} and θ_{v}, and dimensionless relative concentration $\Gamma_{\mathrm{m,v}}$, as well as their dimensionless derivatives. These dimensionless variables constitute whole unknown variables of the governing equations; (ii) All physical properties in Eqs. (28)–(34) exist in form of the dimensionless physical property factors, such as $\frac{1}{\rho_{\mathrm{l}}}\frac{\mathrm{d}\rho_{\mathrm{l}}}{\mathrm{d}\eta_{\mathrm{l}}}$, $\frac{1}{\rho_{\mathrm{m}}}\frac{\mathrm{d}\rho_{\mathrm{m}}}{\mathrm{d}\eta_{\mathrm{v}}}$, $\frac{1}{\mu_{\mathrm{l}}}\frac{\mathrm{d}\mu_{\mathrm{l}}}{\mathrm{d}\eta_{\mathrm{l}}}$, $\frac{1}{\mu_{\mathrm{m}}}\frac{\mathrm{d}\mu_{\mathrm{m}}}{\mathrm{d}\eta_{\mathrm{v}}}$, $\frac{1}{\lambda_{\mathrm{l}}}\frac{\mathrm{d}\lambda_{\mathrm{l}}}{\mathrm{d}\eta_{\mathrm{l}}}$, $\frac{1}{\lambda_{\mathrm{m}}}\frac{\mathrm{d}\lambda_{\mathrm{m}}}{\mathrm{d}\eta_{\mathrm{v}}}$, $\frac{\nu_{\mathrm{l,s}}}{\nu_{\mathrm{l}}}$, $\frac{\nu_{\mathrm{m},\infty}}{\nu_{\mathrm{m}}}$, $\frac{\mu_{\mathrm{l,s}}}{\mu_{\mathrm{l}}}$, $\frac{\mu_{\mathrm{m},\infty}}{\mu_{\mathrm{m}}}$, $\frac{T_{\infty}-273}{T_{\mathrm{s}}-T_{\infty}}$, $\frac{\rho_{\mathrm{l}}-\rho_{\mathrm{m},\infty}}{\rho_{\mathrm{l,w}}-\rho_{\mathrm{m},\infty}}$, $\frac{\rho_{\mathrm{m}}-\rho_{\mathrm{m},\infty}}{\rho_{\mathrm{m,s}}-\rho_{\mathrm{m},\infty}}$, etc.; (iii) Eqs. (28)–(34) involve Prandtl numbers Pr_{l} and Pr_{m}, as well as the local Shcidt number $Sc_{\mathrm{m},\infty}$. In fact, both Prandtl number and Schnidt number are also dimensionless physical property factors.

Here, it is useful to present the mathematical models for the related condensation on the inclined surface. As presented in Shang [5], 2006, Chapters 9 and 15, for free film flows on an inclined surface, the only actions that need to be taken involve replacing the gravitation acceleration g in the governing partial differential equations together with the equations for assumed dimensionless variables, Eqs. (2), (5), (18), (20), (21), (23), (25) and (26) by $g\cos\alpha$. Then, all transformed dimensionless Eqs. (28)–(43) of the film condensation for the vertical case are completely suitable to those for the inclined case.

3. Treatment of variable physical properties

As illustrated in Shang [5], fluid variable physical properties have significant impacts on free film flows and heat transfer. As a result, they need to be appropriately treated to ensure accurate and reliable solution of the governing equations. For the film condensation from pure vapor, temperature-dependent physical properties should be treated, while for the film condensation from the vapor–gas mixture, besides the above treatments, the additional concentration-dependent physical properties of vapor–gas mixture should be dealt with also.

3.1. Treatment of temperature-dependent physical properties of liquid film

For treatment of the temperature-dependent physical properties of liquid film, the polynomial approach reported in [5] is used, and the related treatment equations are omitted here to save space.

3.2. Treatment of concentration-dependent physical properties of vapor–gas mixture film

For density

Suitable treatment of the concentration-dependent densities of vapor–gas mixture film is important for correct determination of the interfacial mass fraction, and then, is a prerequisite for the correct prediction of the interfacial vapor condensate saturation temperature. In the research undertaken to date, there has been an absence of rigorous treatment of the concentration-dependent densities for the study on the film condensation from the vapor–gas mixture. In order to address this gap, the authors have derived the following equations for the rigorous expression of the concentration-dependent densities in the vapor–gas mixture:

$$\rho_{m,v} = \frac{C_{m,v}\rho_v\rho_g}{(1-C_{m,v})\rho_v + C_{m,v}\rho_g} \tag{44}$$

$$\rho_{m,g} = \frac{(1-C_{m,v})\rho_v\rho_g}{C_{m,v}\rho_g + (1-C_{m,v})\rho_v} \tag{45}$$

$$\rho_m \equiv \rho_{m,v} + \rho_{m,g} = \frac{\rho_v\rho_g}{(1-C_{m,v})\rho_v + C_{m,v}\rho_g} \tag{46}$$

where $C_{m,v} = (C_{m,vs} - C_{m,v\infty})\Gamma_{m,v} + C_{m,v\infty}$

Here, $\rho_{m,v}$ and $\rho_{m,g}$ are vapor and gas local densities in vapor–gas mixture respectively, which depend on the vapor mass fraction $C_{m,v}$, while, ρ_v and ρ_g denote the vapor and gas densities, respectively. The derivation processes for Eqs. (44)–(46) are omitted here to save space.

With Eqs. (44), (22), (23) and (27), the expression of the density factor $\frac{1}{\rho_m}\frac{d\rho_m}{d\eta_v}$ in Eqs. (31), (33) and (34) for the vapor–gas mixture film is derived and shown as

$$\begin{aligned}\frac{1}{\rho_m}\frac{d\rho_m}{d\eta_v} = {} & \frac{\frac{1}{\rho_g}\frac{d\rho_g}{d\eta_v} + \frac{1}{\rho_v}\frac{d\rho_v}{d\eta_v}}{(1-C_{m,v})\frac{\rho_m}{\rho_g} + C_{m,v}\frac{\rho_m}{\rho_v}} \\ & - \frac{\rho_v\rho_g}{\left((1-C_{m,v})\rho_v + C_{m,v}\rho_g\right)^2} \\ & \times \left[(1-C_{m,v})\frac{1}{\rho_v}\frac{d\rho_v}{d\eta_v}\frac{\rho_v}{\rho_m}\right. \\ & \left. - \frac{\rho_v-\rho_g}{\rho_m}(C_{v,ws} - C_{v,w\infty})\frac{d\Gamma_{m,v}}{d\eta_v} + C_{m,v}\frac{1}{\rho_g}\frac{d\rho_g}{d\eta_v}\frac{\rho_g}{\rho_m}\right]\end{aligned} \tag{47}$$

where $C_{m,v} = (C_{m,vs} - C_{m,v\infty})\Gamma_{m,v} + C_{m,v\infty}$.

For other physical properties

For the expressions of other concentration-dependent physical properties of vapor–gas mixture, such as absolute viscosity, thermal conductivity, specific heat and Prandtl number, there has not been an appropriate treatment method developed due to the absence of experimental data. Here, we use the following weighted-sums to approximately describe them respectively:

$$\mu_m = C_{m,v}\mu_v + (1-C_{m,v})\mu_g \tag{48}$$

$$\lambda_m = C_{m,v}\lambda_v + (1-C_{m,v})\lambda_g \tag{49}$$

$$c_{p_m} = C_{m,v}c_{p_v} + (1-C_{m,v})c_{p_g} \tag{50}$$

$$Pr_m = C_{m,v}Pr_v + (1-C_{m,v})Pr_g \tag{51}$$

where $C_{m,v} = (C_{m,vs} - C_{m,v\infty})\Gamma_{m,v} + C_{m,v\infty}$

Here, μ_v, λ_v, c_{p_v} and Pr_v denote the absolute viscosity, thermal conductivity, specific heat, and Prandtl number of vapor, while, μ_g, λ_g, c_{p_g} and Pr_g denote those physical properties of gas, respectively.

Similar to the derivation for Eq. (47),expressions of the viscosity factor $\frac{1}{\mu_m}\frac{d\mu_m}{d\eta_v}$ in Eq. (32) and the thermal conductivity factor $\frac{1}{\lambda_m}\frac{d\lambda_m}{d\eta_v}$ in Eq. (33) for the vapor–gas mixture film are obtained, and shown as follows respectively:

$$\begin{aligned}\frac{1}{\mu_m}\frac{d\mu_m}{d\eta_v} = {} & C_{m,v}\frac{1}{\mu_v}\frac{d\mu_v}{d\eta_v}\cdot\frac{\mu_v}{\mu_m} + (1-C_{m,v})\frac{1}{\mu_g}\frac{d\mu_g}{d\eta_v}\cdot\frac{\mu_g}{\mu_m} \\ & + (C_{m,vs} - C_{m,v\infty})\frac{\mu_v-\mu_g}{\mu_m}\frac{d\Gamma_{m,v}}{d\eta_v}\end{aligned} \tag{52}$$

$$\begin{aligned}\frac{1}{\lambda_m}\frac{d\lambda_m}{d\eta_v} = {} & C_{m,v}\frac{1}{\lambda_v}\frac{d\lambda_v}{d\eta_v}\cdot\frac{\lambda_v}{\lambda_m} + (1-C_{m,v})\frac{1}{\lambda_g}\frac{d\lambda_g}{d\eta_v}\cdot\frac{\lambda_g}{\lambda_m} \\ & + (C_{m,vs} - C_{m,v\infty})\frac{\lambda_v-\lambda_g}{\lambda_m}\frac{d\Gamma_{m,v}}{d\eta_v}\end{aligned} \tag{53}$$

where $C_{m,v} = (C_{m,vs} - C_{m,v\infty})\Gamma_{m,v} + C_{m,v\infty}$

3.3. Treatment of temperature-dependent physical properties of vapor–gas mixture

For treatment of the related temperature-dependent physical properties in Eqs. (47), (52) and (53), the temperature parameter method [5] is applied, and the related vapor and gas physical property factors are expressed as follows, respectively:

For density factors

$$\frac{1}{\rho_v}\frac{d\rho_v}{d\eta_v} = -\frac{(T_s/T_\infty - 1)d\theta_v/d\eta_v}{(T_s/T_\infty - 1)\theta_v + 1} \tag{54}$$

$$\frac{1}{\rho_g}\frac{d\rho_g}{d\eta_v} = -\frac{(T_s/T_\infty - 1)d\theta_v/d\eta_v}{(T_s/T_\infty - 1)\theta_v + 1} \tag{55}$$

For absolute viscosity factors

$$\frac{1}{\mu_v}\frac{d\mu_v}{d\eta_v} = \frac{n_{\mu,v}(T_s/T_\infty - 1)d\theta_v/d\eta_v}{(T_s/T_\infty - 1)\theta_v + 1} \tag{56}$$

$$\frac{1}{\mu_g}\frac{d\mu_g}{d\eta_v} = \frac{n_{\mu,g}(T_s/T_\infty - 1)d\theta_v/d\eta_v}{(T_s/T_\infty - 1)\theta_v + 1} \tag{57}$$

For thermal conductivity factors

$$\frac{1}{\lambda_v}\frac{d\lambda_v}{d\eta_v} = \frac{n_{\lambda,v}(T_s/T_\infty - 1)d\theta_v/d\eta_v}{(T_s/T_\infty - 1)\theta_v + 1} \tag{58}$$

$$\frac{1}{\lambda_g}\frac{d\lambda_g}{d\eta_v} = \frac{n_{\lambda,g}(T_s/T_\infty - 1)d\theta_v/d\eta_v}{(T_s/T_\infty - 1)\theta_v + 1} \tag{59}$$

Here, $n_{\mu,v}$ and $n_{\mu,g}$ are viscosity parameters of vapor and gas respectively, while, $n_{\lambda,v}$ and $n_{\lambda,g}$ are thermal conductivity parameters of vapor and gas respectively.

4. Numerical solutions

4.1. Calculation procedure

Satisfying the whole set of the interfacial matching conditions of the governing equations for the film condensation from the vapor–gas mixture is more difficult than that from the pure vapor. For overcoming this difficult point, on the basis of our previous studies [21,22] for numerical calculation of the film condensation from pure vapor, we present the following procedural steps of numerical calculations on the film condensation from the vapor–gas mixture:

Step 1: Calculation for liquid film

First, the solution of Eqs. (28)–(30) for liquid film are assumed to be without shear force at the liquid–vapor

interface. For this case, the boundary condition (38) is changed into Eq. (60) at the

$$\left(\frac{dW_{xl}}{d\eta_l}\right)_{\eta_l=\eta_{l,\delta}} = 0 \tag{60}$$

beginning of the calculation, and the initial values of the condensate liquid film thickness $\eta_{l\delta}$ and condensate liquid velocity component $W_{xl,s}$ are assumed. Eqs. (35), (40) and (60) are taken as the boundary conditions of the liquid film, and Eqs. (28)–(30) are solved by a shooting method with fifth-order Runge-Kutta integration.

Step 2: Calculation for vapor–gas mixture film

First, with the numerical solutions, $W_{xl,s}$ and $W_{yl,s}$ calculated from the first step, the boundary values $W_{xv,s}$ and $W_{yv,s}$ are evaluated by Eqs. (36) and (37), respectively. Then, with the boundary conditions (40), (41) and (43) and the above values of $W_{xv,s}$ and $W_{yv,s}$, Eqs. (31)–(34) for vapor–gas mixture film are calculated by using the shooting method with seventh-order Runge-Kutta integration.

Step 3: Judgment on the convergence of the numerical calculation

Eqs. (38), (39) and (42) are taken as judgment equations for verification of the convergence of the solutions. By means of these judgment equations, the calculation is iterated with appropriate change for the values $W_{xl,s}$ and $\eta_{l\delta}$. In each iteration, step 1 for calculations of Eqs. (28)–(30) for liquid film, and step 2 for calculation of Eqs. (31)–(34) for vapor–gas mixture film are done successively. For solving the very strong nonlinear problem, a variable mesh approach is applied to the numerical calculation programs.

4.2. Determination of interfacial vapor condensate saturation temperature

Accurate determination of the interfacial vapor condensate saturated temperature is a prerequisite for reliable prediction of the film condensation of vapor in presence of no-condensable gas. However, the interfacial vapor saturated temperature depends on the interfacial vapor partial pressure, and, ultimately, on the interfacial vapor mass fraction $C_{m,vs}$. Furthermore, the value of $C_{m,vs}$ for the film condensation from the vapor–gas mixture is an unknown variable before the calculation. To date, there has been lack of rigorous analysis on this area. This study addresses this gap.

Let us take the water vapor–air mixture as an example for this investigation. We recommend the following equation for expression of the water vapor condensate saturated temperature T_s with its interfacial vapor mass fraction $C_{m,vs}$:

$$T_s = 373 \cdot C_{m,vs}^{0.063} \tag{61}$$

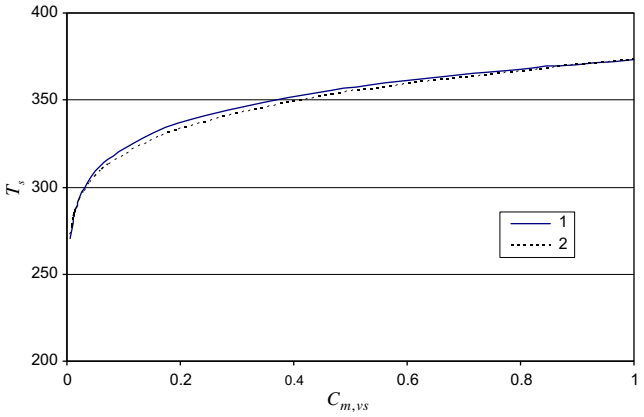

Fig. 2. Water vapor condensate saturated temperature T_s with the corresponding interfacial vapor mass fraction $C_{m,vs}$ (Line 1: predicted value with Eq. (61); Line 2: experimental value from [23]).

The values of T_s are obtained from Eq. (61) and plotted in Fig. 2 with the related interfacial gas mass fraction $C_{m,vs}$. Compared with the typical experimental data [23], the maximum deviation predicted by Eq. (61) is less than 1.1% for saturated water vapor.

From the governing ordinary Eqs. (28)–(34) and their boundary conditions, Eqs. (35)–(43), it will be expected that the interfacial vapor mass fraction $C_{m,vs}$ and the interfacial vapor condensate saturated temperature T_s, together with the velocity, temperature and concentration fields, and heat and mass transfer are solutions of the system of the mathematical model. These, in turn, are dependent on the given wall temperatures T_w, bulk temperature T_∞, and the bulk concentration condition, $C_{m,v\infty}$ (or $C_{m,g\infty}$) for the film condensation from the vapor–gas mixture.

4.3. Numerical solutions

In this present work, the laminar free film condensation of water vapor in presence of air is taken as an example for the numerical calculation. The bulk vapor–gas mixture temperature is set as $T_\infty = 373$ K. According to Shang[5], Chapter 4, we take the viscosity parameter and thermal conductivity parameter as $n_{\mu,v} = 1.04$ and $n_{\lambda,v} = 1.185$, respectively for water vapor; and $n_{\mu,g} = 0.68$ and $n_{\lambda,g} = 0.81$ respectively, for air. The other related physical values for water vapor and air are also taken from [5], but omitted here to save space.

For laminar free film condensation of water vapor in presence of air, a system of numerical calculations have been successfully carried out for different wall temperatures T_w and bulk water vapor mass fraction $C_{m,v\infty}$ at $T_\infty = 373$ K. It is interesting to note that the calculated results show that the interfacial water vapor mass fraction $C_{v,ws}$ is exactly half of the bulk water vapor mass fraction $C_{v,w\infty}$, and only depends on $C_{v,w\infty}$ for the film condensation from the water vapor–air mixture. The system of calculated results for velocity and temperature profiles of condensate water film and velocity profiles of water

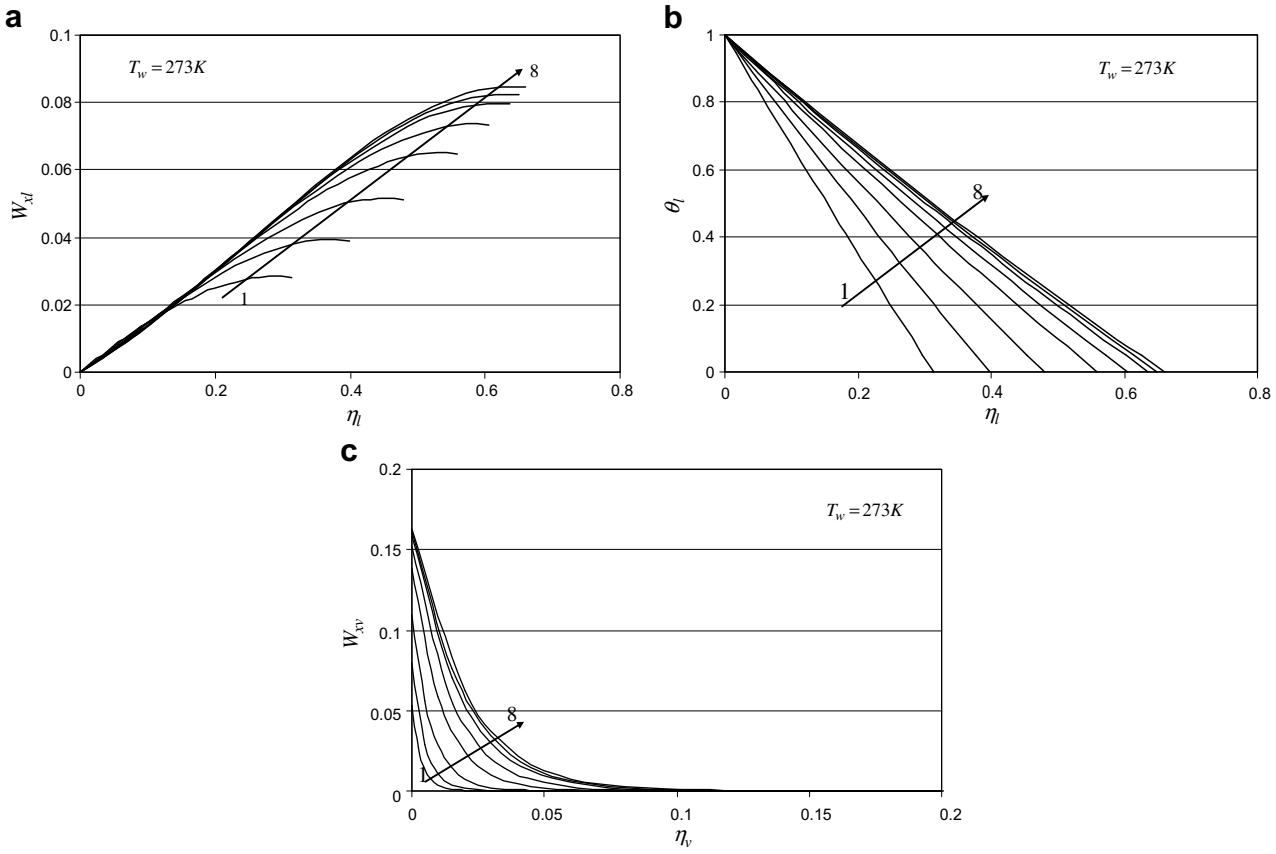

Fig. 3. Numerical results of (a) velocity component W_{xl} profiles and (b) temperature θ_l profiles of liquid film, and (c) velocity component W_{xv} profiles of vapor–gas mixture film for laminar free film condensation of water vapor in presence of air at $T_w = 273$ K and $T_\infty = 373$ K (Lines 1–8 for $C_{m,v\infty} = 0.05$, 0.1, 0.2, 0.4, 0.6, 0.8, 0.9 and 0.99).

vapor–air mixture film are obtained and plotted in Figs. 3–5 respectively. From these Figures, it is easy to find the following effect regulations of the given conditions, wall temperatures T_w and bulk gas mass fraction $C_{m,g\infty}$ on the free film condensation from the vapor–gas mixture.

An increase of the bulk gas mass fraction $C_{m,g\infty}$ will cause a decrease in the condensate liquid film velocity and thickness, and a decrease of the velocity of the vapor–gas mixture film. This, in turn, leads to a weakened condensate process. Similarly, an increase of the bulk gas mass fraction $C_{m,g\infty}$ will cause a decrease in the concentration boundary layer thickness. An increase of wall temperature T_w causes a decrease of the condensate film velocity and thickness. Anyway, an increase of wall temperature T_w causes an increase in the thicknesses of the velocity and concentration boundary layers of the vapor–gas mixture film.

4.4. Critical vapor mass fraction

The above calculation results demonstrate that a decrease in the bulk vapor mass fraction $C_{m,v\infty}$ causes a decrease in the vapor interfacial saturated temperature, and causes the decrease of the wall sub-cooled temperature. If a decreased vapor mass fraction $C_{m,v\infty}$ is less than a special value $C^*_{m,v\infty}$ ($C^*_{m,v\infty}$ is corresponding to $t_s - t_w \to 0$), the wall subcooled temperature will be less than zero, i.e. $t_s - t_w < 0$, and the condensation will never happen theoretically. On the contrary, if the bulk vapor mass fraction $C_{m,v\infty}$ is larger than the special value $C^*_{m,v\infty}$, the wall subcooled temperature will be larger than zero, i.e. $t_s - t_w > 0$, and then, the condensation will happen theoretically. This special bulk vapor mass fraction $C^*_{m,v\infty}$ describes a critical value of $C_{m,v\infty}$ for the film condensation from the vapor–gas mixture; it is defined here as the critical bulk vapor mass fraction. Obviously, when $C_{m,v\infty} > C^*_{m,v\infty}$, the film condensation will exist, while, if $C_{m,v\infty} < C^*_{m,v\infty}$, the film condensation will never happen.

In this present work, the critical vapor mass fraction $C^*_{m,v\infty}$ is obtained for the free film condensation from water vapor–air mixture, and plotted in Fig. 6 with the relative temperature $\frac{t_\infty - t_w}{t_\infty}$. The upper portion of the critical line is the condensable region where the condensation will exist; but below the critical line is the non-condensable region where the condensation will never happen. For the special vapor, the value of $C^*_{m,v\infty}$ depends on the wall and bulk temperatures. Increasing the wall temperature causes the increase of the critical vapor mass fraction $C^*_{m,v\infty}$.

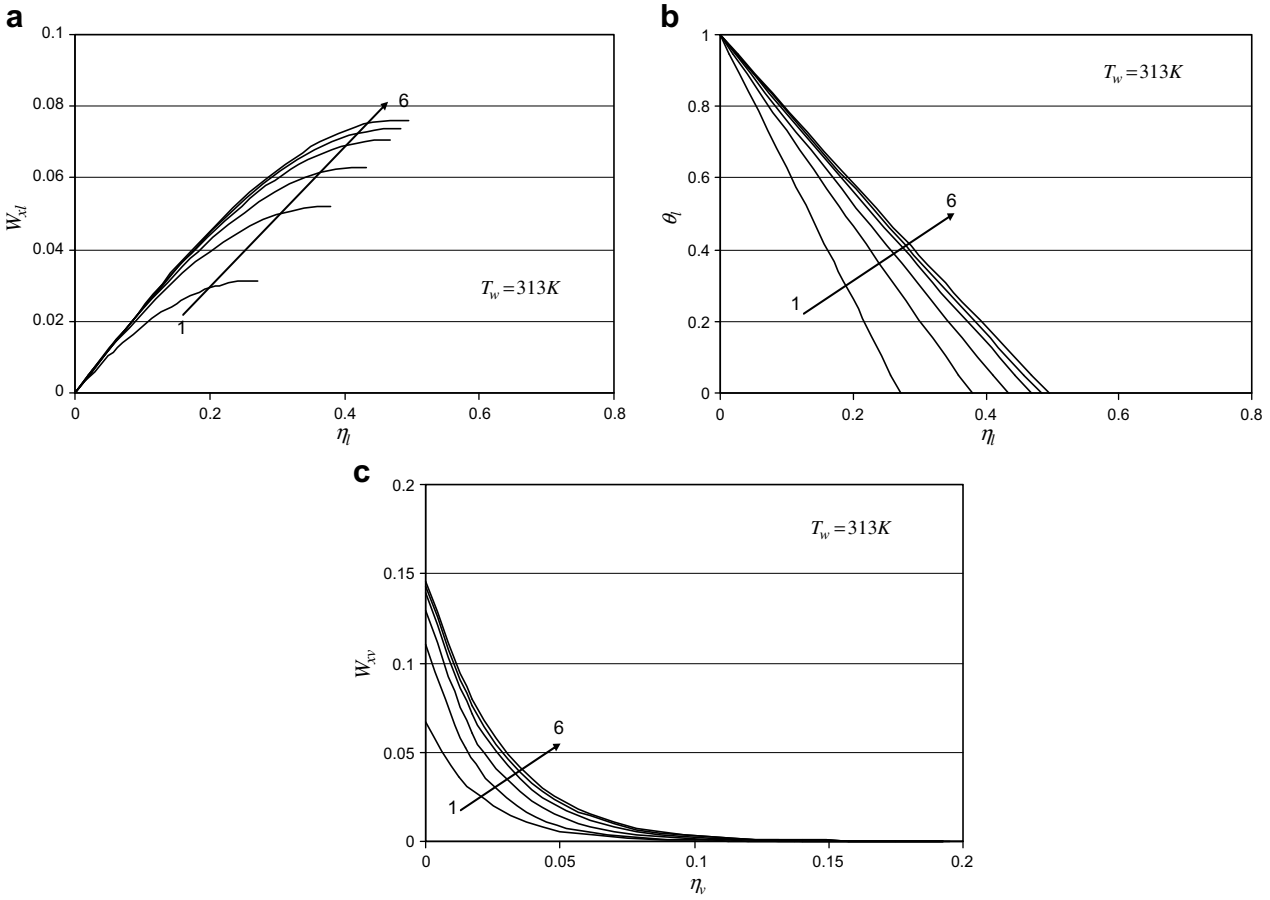

Fig. 4. Numerical results of (a) velocity component W_{xl} profiles and (b) temperature θ_l profiles of liquid film, and (c) velocity component W_{xv} profiles of vapor–gas mixture film for laminar free film condensation of water vapor in presence of air at $T_w = 313$ K and $T_\infty = 373$ K (Lines 1–6 for $C_{m,v\infty} = 0.2$, 0.4, 0.6, 0.8, 0.9 and 0.99).

5. Heat transfer

5.1. Heat transfer analysis

The local heat transfer rate q_x of the film condensation at position x per unit area on the plate can be calculated by applying Fourier's law as $q_x = -\lambda_{l,w}\left(\frac{\partial T_l}{\partial y_l}\right)_{y_l=0}$. As presented in Shang [5], Chapter 12, the following equations on heat transfer for free film condensation from vapor–gas mixture can be obtained:

$$q_x = -\lambda_{l,w}(T_s - T_w)\left(\frac{1}{4}Gr_{xl,s}\right)^{1/4} x^{-1}\left(\frac{d\theta_l}{d\eta_l}\right)_{\eta_l=0} \tag{62}$$

$$\alpha_x = -\lambda_{l,w}\left(\frac{1}{4}Gr_{xl,s}\right)^{1/4} x^{-1}\left(\frac{d\theta_l}{d\eta_l}\right)_{\eta_l=0} \tag{63}$$

$$Nu_{xl,w} = \left(\frac{1}{4}Gr_{xl,s}\right)^{1/4}\left(\frac{d\theta_l}{d\eta_l}\right)_{\eta_l=0} \tag{64}$$

where α_x and $Nu_{xl,w}$ are local heat transfer coefficient and local Nusselt number, defined as $q_x = \alpha_x(T_s - T_w)$ and $Nu_{xl,w} = \frac{\alpha_x x}{\lambda_{l,w}}$ respectively. Here, $\left(\frac{d\theta_l}{d\eta_l}\right)_{\eta_l=0}$ is the dimensionless temperature gradient on the plate, to simplify the presentation, the temperature gradient. The following average values can be expressed for engineering application:

$$\bar{\alpha}_x = -\frac{4}{3}\lambda_{l,w}\left(\frac{1}{4}Gr_{xl,s}\right)^{1/4} x^{-1}\left(\frac{d\theta_l}{d\eta_l}\right)_{\eta_l=0} \tag{65}$$

$$\overline{Nu}_{xl,w} = -\frac{4}{3}\left(\frac{1}{4}Gr_{xl,s}\right)^{1/4} x^{-1}\left(\frac{d\theta_l}{d\eta_l}\right)_{\eta_l=0} \tag{66}$$

where $\overline{\alpha_x}$ and $\overline{Nu}_{xl,w}$ are average heat transfer coefficient and average Nusselt number defined as $Q_x = \bar{\alpha}_x(T_s - T_w)\cdot b\cdot x$ and $\overline{Nu}_{xl,w} = \frac{\bar{\alpha}_x x}{\lambda_{l,w}}$ respectively. Here, Q_x is total heat transfer rate.

If we set $(q_x)_{C_{m,v\infty}=1}$ as local heat transfer rater with $C_{m,v\infty} = 1$ corresponding to the film condensation of pure vapor, then, $\frac{q_x}{(q_x)_{C_{m,v\infty}=1}}$ is the heat transfer ratio of film condensation from the vapor–gas mixture to that from pure vapor, for short, heat transfer ratio. From Eq. (62), the heat transfer ratio can be expressed as

$$\frac{q_x}{(q_x)_{C_{m,v\infty}=1}} = \frac{\Delta T_w}{(\Delta T_w)_{C_{m,v\infty}=1}}\cdot\left[\frac{Gr_{xl,s}}{(Gr_{xl,s})_{C_{m,v\infty}=1}}\right]^{1/4}\frac{\left(\frac{d\theta_l}{d\eta_l}\right)_{\eta_l=0}}{\left[\left(\frac{d\theta_l}{d\eta_l}\right)_{\eta_l=0}\right]_{C_{m,v\infty}=1}} \tag{67}$$

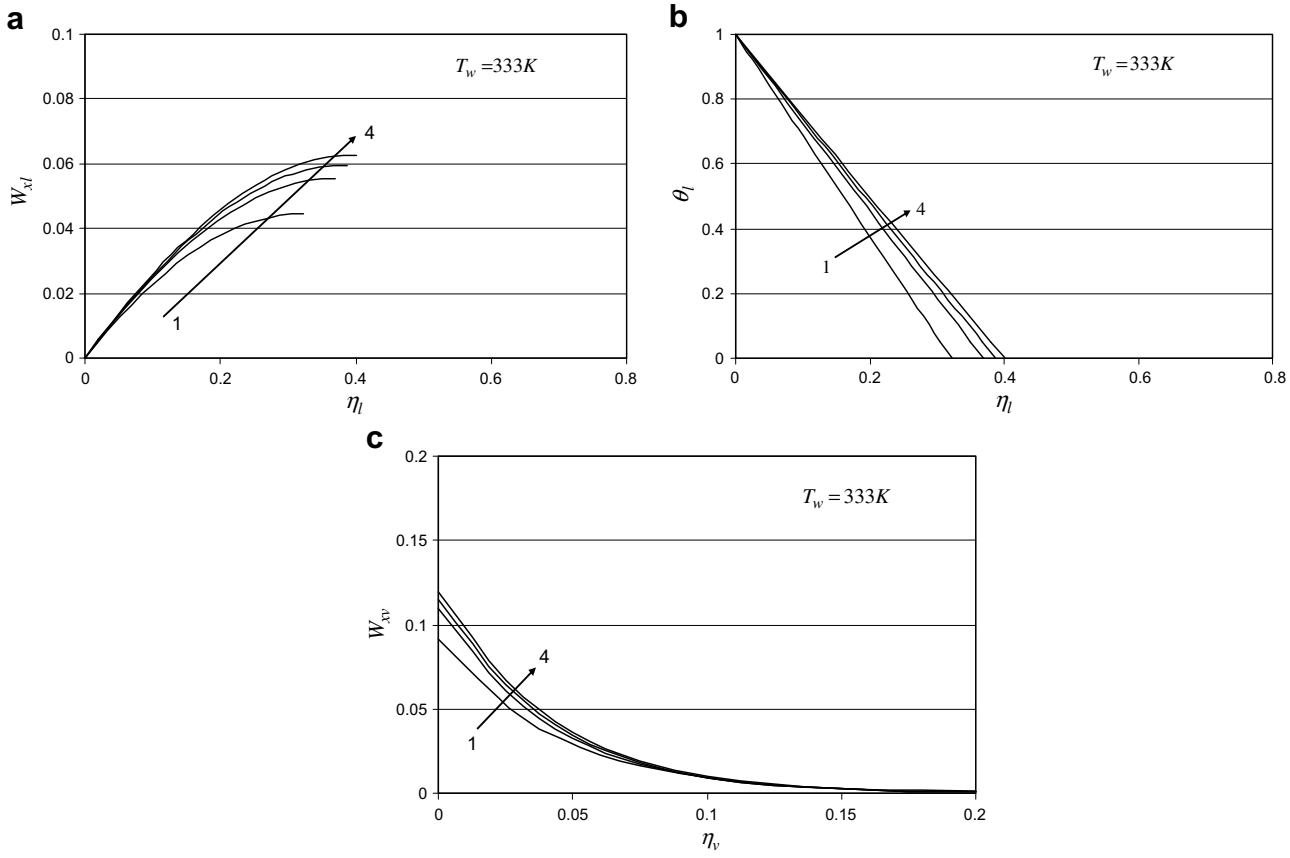

Fig. 5. Numerical results of (a) velocity component W_{xl} profiles and (b) temperature θ_l profiles of liquid film, and (c) velocity component W_{xv} profiles of vapor–gas mixture film for laminar free film condensation of water vapor in presence of air at $T_w = 333$ K and $T_\infty = 373$ K (Lines 1–4 for $C_{m,v\infty} = 0.6$, 0.8, 0.9 and 0.99).

Here, $\frac{\Delta T_w}{(\Delta T_w)_{C_{m,v\infty}=1}} = \frac{T_s - T_w}{(T_s)_{C_{m,v\infty}=1} - T_w}$ is the ratio of wall sub-cooled temperature $T_s - T_w$ with any bulk vapor mass fraction $C_{m,v\infty}$ to that with $C_{m,v\infty} = 1$, for short, wall sub-cooled temperature ratio. Similarly, $\left[\frac{Gr_{xl,s}}{(Gr_{xl,s})_{C_{m,v\infty}=1}}\right]^{1/4}$ and $\frac{\left(\frac{d\theta_l}{d\eta_l}\right)_{\eta_l=0}}{\left[\left(\frac{d\theta_l}{d\eta_l}\right)_{\eta_l=0}\right]_{C_{m,v\infty}=1}}$ can be called local Grashof number ratio and temperature gradient ratio, respectively.

In this work, a system of ratios of $\frac{\Delta T_w}{(\Delta T_w)_{C_{m,v\infty}=1}}$, $\left[\frac{Gr_{xl,s}}{(Gr_{xl,s})_{C_{m,v\infty}=1}}\right]^{1/4}$ and $\frac{\left(\frac{d\theta_l}{d\eta_l}\right)_{\eta_l=0}}{\left[\left(\frac{d\theta_l}{d\eta_l}\right)_{\eta_l=0}\right]_{C_{m,v\infty}=1}}$ are obtained for the laminar free film condensation of water vapor in presence of air, and plotted in (a), (b) and (c) of Fig. 7, respectively, with variation of T_w and $C_{m,v\infty}$.

5.2. Effect of bulk mass fraction and wall temperature

A series of heat transfer ratios are evaluated by using Eq. (67) and plotted in (d) of Fig. 7. As illustrated, decreasing the bulk vapor mass fraction $C_{m,v\infty}$ (or increasing the bulk gas mass fraction $C_{m,g\infty}$) causes the decrease of the heat transfer ratio to accelerate. Similarly, for a special bulk vapor mass fraction, an increase of the wall temperature T_w (or decreasing the wall sub-cooled temperature $T_s - T_w$) will cause a decrease in the condensate heat transfer ratio. These effect regulations on heat transfer are identical to those on the condensate liquid film velocity and thickness reported in Section 4.3. Meanwhile, it is found that the wall subcooled temperature ratios $\frac{\Delta T_w}{(\Delta T_w)_{C_{m,v\infty}=1}}$ dominate the heat transfer ratios $\frac{q_x}{(q_x)_{C_{m,v\infty}=1}}$ in value.

5.3. Comparison with the previous results

Let us compare the present results in (d) of Fig. 7 with those in (a) of Fig. 8 cited from Ref. [6]. This comparison illustrates that their calculated results are quite different. The results in (d) of Fig. 7 from the present study shows that increase of the wall temperature (or decrease of the wall sub-cooled temperature $T_s - T_w$) causes the decrease of condensate heat transfers ratio at an accelerated pace. However, the results in (a) of Fig. 8 shows the opposite variation. The results in (b) of Fig. 8 presents the calculated values identically transformed from those in (d) of Fig. 7 to facilitate the comparison. Let us analyze the reasons behind the differences.

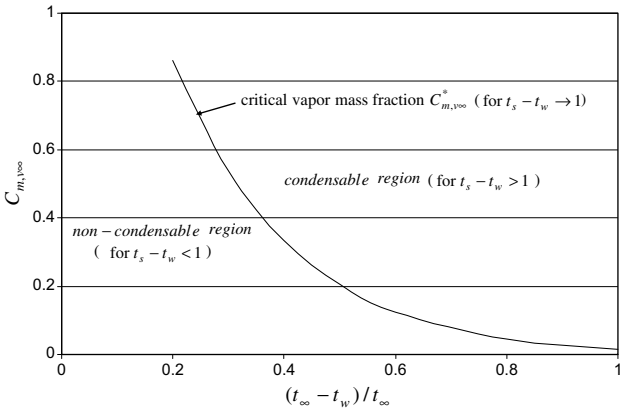

Fig. 6. Critical vapor mass fraction $C^*_{m,v\infty}$, condensable region and non-condensable region with the relative temperature $\frac{t_\infty - t_w}{t_\infty}$ for water vapor–air mixture at $t_\infty = 100$ °C.

Eq. (67) showed that for special bulk gas mass fraction, the condensate heat transfer ratio $\frac{q_x}{(q_x)_{C_{m,v\infty}=1}}$ is proportional to the wall subcooled temperature ratio $\frac{\Delta T_w}{(\Delta T_w)_{C_{m,v\infty}=1}} = \frac{T_s - T_w}{(T_s)_{C_{m,v\infty}=1} - T_w}$. Moreover, for a special bulk gas mass fraction,, increasing the wall temperature will cause a decrease of the wall sub-cooled temperature ratio $\frac{T_s - T_w}{(T_s)_{C_{m,v\infty}=1} - T_w}$ faster and faster. This is the reason why the heat transfer ratio will decrease with an increase in the wall temperature (or a decrease in the wall sub-cooled temperature) for the special bulk gas mass fraction. Therefore, the opposite variation of condensate heat transfer ratio as presented in (a) of Fig. 8 is incorrect, and it must be caused by the incorrect determination of the interfacial vapor condensate saturation temperature.

There remain two other difficult points which need to be addressed to enable correct prediction of the condensate heat transfer from the vapor–gas mixture: reliable analysis of the concentration-dependent densities of the vapor–gas mixture film and rigorous satisfaction of all seven interfacial boundary conditions. This present study resolves the misunderstandings and gaps which currently exist in the research literature.

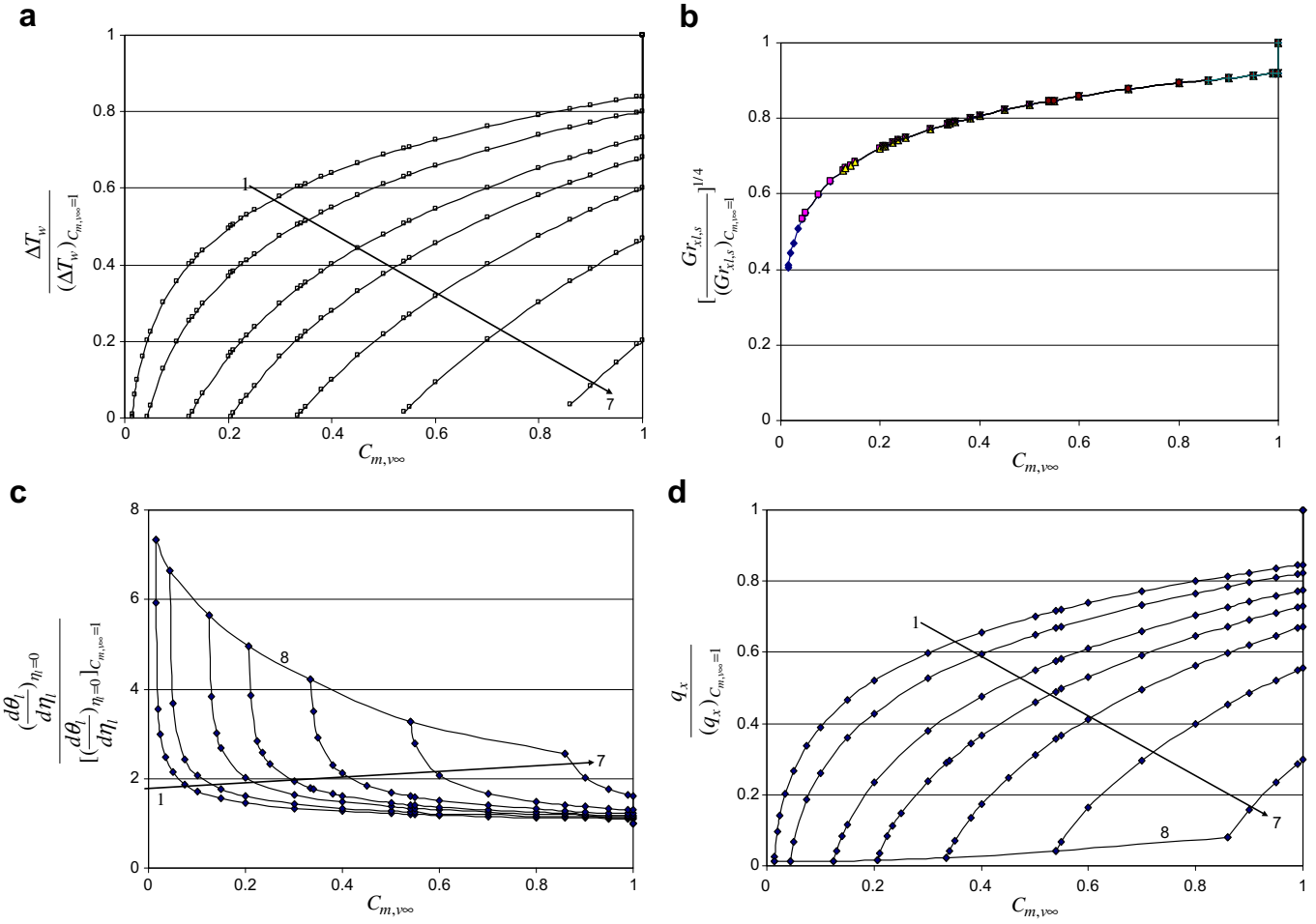

Fig. 7. Results of (a) wall sub-cooled temperature ratio, (b) local Grashof number ratio, (c) temperature gradient ratio, and (d) heat transfer ratio with variation of T_w and $C_{m,v\infty}$ at $T_\infty = 373$ K (Lines 1–7 for $T_w = 273$, 293, 313, 323, 333, 343 and 353 K; Line 8 is critical line corresponding to critical vapor mass fraction $C^*_{m,v\infty}$).

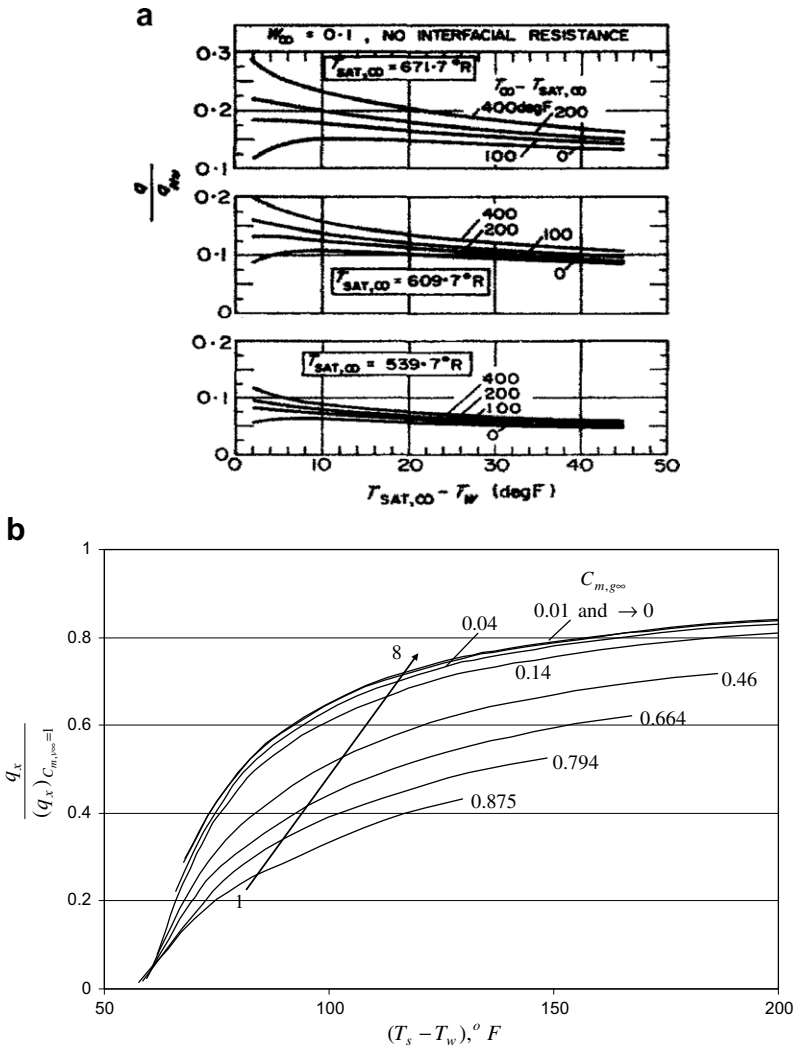

Fig. 8. Comparison of heat transfer ratio results on laminar free film condensation from water vapor–air mixture: (a) cited from Minkowycz and Sparrow [6] ($\frac{q}{q_{Nu}}$, $T_{sat,\infty}$ and W_∞ should be $\frac{q_x}{(q_x)_{C_{m,v\infty}=1}}$, T_s, and $C_{m,g\infty}$, respectively), and the temperature values 671.7, 609.7 and 539.7 °R equal 100, 65.57 and 26.67 °C, respectively; (b) identical expressions to (d) of Fig. 7 (lines 1–8: for $C_{m,g\infty} = 0.875$, 0.794, 0.664, 0.46, 0.14, 0.04, 0.01 and →0 respectively).

6. Mass transfer

6.1. Mass transfer analysis

As presented in Shang[5], Chapter 12, the local condensate mass flow rate g_x entering the liquid film at position x related to per unit area of the plate is derived for the film condensation from the vapor–gas mixture. This is expressed as

$$g_x = \mu_{l,s} x^{-1} \left(\frac{1}{4} Gr_{xl,s}\right)^{1/4} \Phi_s \tag{68}$$

where Φ_s is the mass flow rate parameter defined as

$$\Phi_s = \eta_{l\delta} W_{xl,s} - 4 W_{yl,s} \tag{69}$$

Here, $\eta_{l\delta}$ is dimensionless condensate liquid film thickness, and $W_{xl,s}$, and $W_{yl,s}$ are interfacial dimensionless condensate liquid velocity components in x and y directions, respectively.

The total mass flow rate G_x entering the liquid film for position $x = 0$ to x with width b of the plate is derived, and expressed as

$$G_x = \frac{4}{3} b \cdot \mu_{l,s} \left(\frac{1}{4} Gr_{xl,s}\right)^{1/4} \Phi_s \tag{70}$$

If we take $(g_x)_{C_{m,v\infty}=1}$ as the condensate mass transfer rate for $C_{m,v\infty} = 1$ actually corresponding to the film condensation of pure vapor, then, $\frac{g_x}{(g_x)_{C_{m,v\infty}=1}}$ is defined as ratio of condensate mass transfer rate from vapor–gas mixture to that from pure vapor. This is referred to as the mass transfer ratio, for short. From Eq. (68), the mass transfer ratio can be expressed as

$$\frac{g_x}{(g_x)_{C_{m,v\infty}=1}} = \frac{\mu_{l,s}}{(\mu_{l,s})_{C_{m,v\infty}=1}} \left[\frac{Gr_{xl,s}}{(Gr_{xl,s})_{C_{m,v\infty}=1}}\right]^{1/4} \frac{\Phi_s}{(\Phi_s)_{C_{m,v\infty}=1}} \tag{71}$$

where the local Grashof number ratio $\left[\frac{Gr_{xl,s}}{(Gr_{xl,s})_{C_{m,v\infty}=1}}\right]^{1/4}$ is defined in Section 5. Here, $\frac{\mu_{l,s}}{(\mu_{l,s})_{C_{m,v\infty}=1}}$ and $\frac{\Phi_s}{(\Phi_s)_{C_{m,v\infty}=1}}$ are named absolute viscosity ratio and mass flow rate parameter ratio, respectively.

6.2. Effect of bulk mass fraction and wall temperature

The evaluated absolute viscosity ratios and mass flow rate parameter ratios are obtained for the free film condensation from the water vapor–air mixture, and plotted in (a) and (b) of Fig. 9 respectively, with the variation of T_w and $C_{m,v\infty}$.

On this basis, the condensate mass flow rate ratios are determined according to Eq. (71), and plotted in (c) of Fig. 9 with the variation of T_w and $C_{m,v\infty}$. It can be seen that decreasing the bulk vapor mass fraction $C_{m,v\infty}$ causes a decrease in the condensate mass flow rate ratio. Meanwhile, an increase of the wall temperature will cause a decrease of the condensate mass flow rate ratio. From (d) of Fig. 7 and (c) of Fig. 9, it is clear that the condensate heat transfer ratios are well identical with the condensate mass transfer ratios. This means that the condensate heat and mass transfers are equivalent in value. However, the heat transfer rate is defined on the plate, and the condensate mass flow rate is defined at the liquid–vapor interface. Such difference in definition causes the very little bit difference between their values. Furthermore, it is found that the mass flow rate parameter ratios $\frac{\Phi_s}{(\Phi_s)_{C_{m,v\infty}=1}}$ dominate the mass transfer ratios $\frac{g_x}{(g_x)_{C_{m,v\infty}=1}}$ in value.

7. Variances in condensations with $C_{m,v\infty} \to 1$ vs $C_{m,v\infty} = 1$

If $(f)_{C_{m,v\infty}}$ is used as the function of $C_{m,v\infty}$ to express the calculated result of the film condensation, then, $(f)_{C_{m,v\infty}\to 1}$ and $(f)_{C_{m,v\infty}=1}$ show the limit value related to $C_{m,v\infty} \to 1$ (i.e. $C_{m,g\infty} \to 0$) and the value of the function for $C_{m,v\infty} = 1$ (i.e. $C_{m,g\infty} = 0$), respectively. Furthermore, $\frac{(q_x)_{C_{m,v\infty}\to 1}}{(q_x)_{C_{m,v\infty}=1}}$ is used to determine the heat transfer ratio of the free film

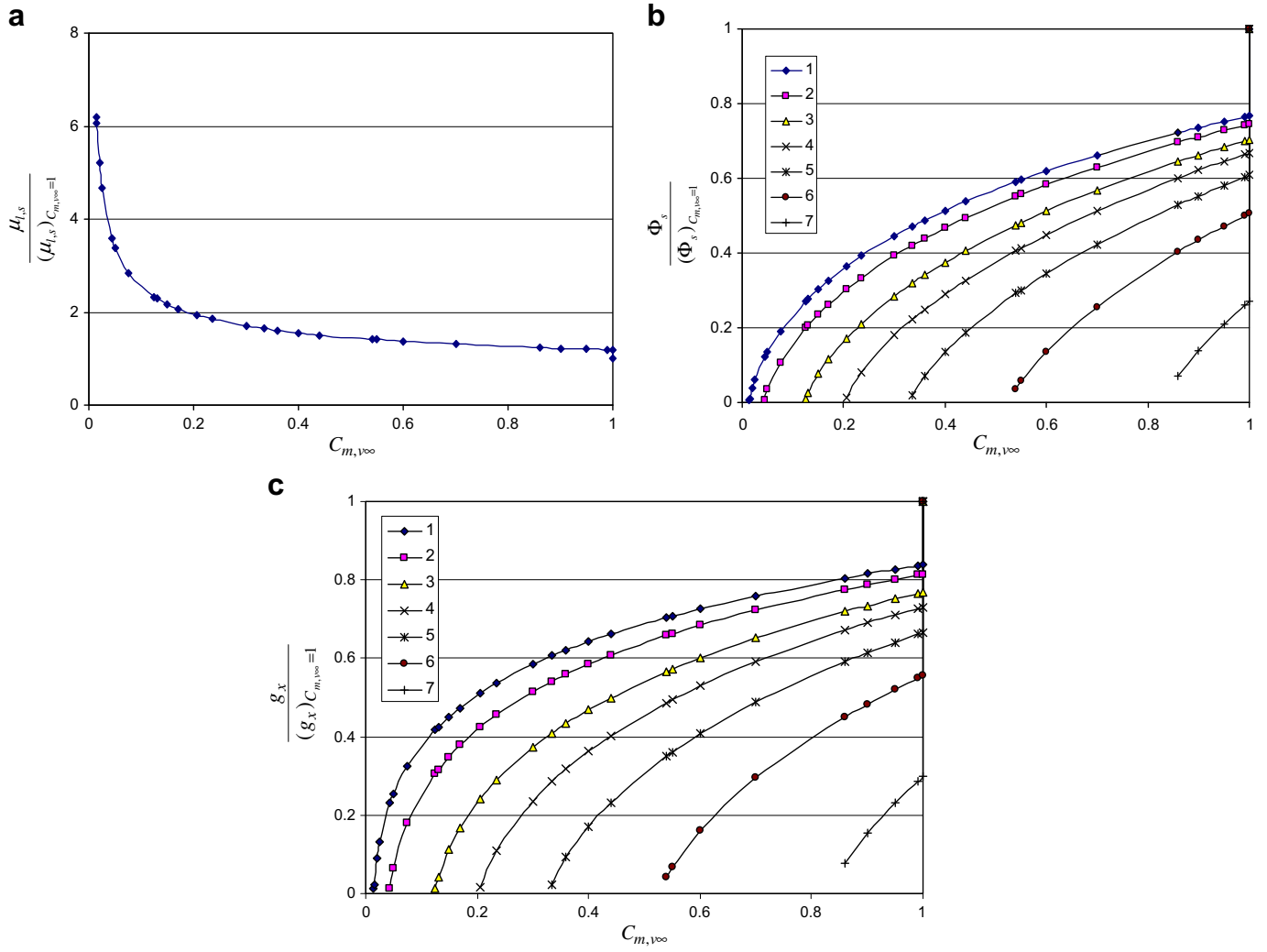

Fig. 9. Results of (a) absolute viscosity ratio, (b) mass flow rate parameter ratio, and (c) condensate mass flow rate ratio with variation of T_w and $C_{m,v\infty}$ for laminar free film condensation from water vapor–air mixture at $T_\infty = 373$ K (Lines 1–7 for $T_w = 273$, 293, 313, 323, 333, 343 and 353 K respectively).

condensation from the vapor–gas mixture for $C_{m,v\infty} \to 1$ (i.e. $C_{m,g\infty} \to 0$) to that for $C_{m,v\infty} = 1$ (i.e. $C_{m,g\infty} = 0$), and plotted as line 8 in (b) of Fig. 8. Obviously, $\frac{(q_x)_{C_{m,v\infty}\to 1}}{(q_x)_{C_{m,v\infty}=1}} \left(= \frac{(q_x)_{C_{m,g\infty}\to 0}}{(q_x)_{C_{m,g\infty}=0}}\right) \neq 1$. It means that the condensate heat transfer is discontinuous at the point $C_{m,v\infty} = 0$. Moreover, an increase of the wall temperature will cause a decrease in the heat and mass transfer ratios.

In fact, the film condensation from the vapor–gas mixture for $C_{m,v\infty} \to 1$ (i.e.$C_{m,g\infty} \to 0$) is quite different from that of pure vapor with $C_{m,v\infty} = 1$ (i.e. $C_{m,g\infty} = 0$), in the condensation mechanism. For the former case with $C_{m,v\infty} \to 1$ (i.e. $C_{m,g\infty} \to 0$), the film condensation at the liquid–vapor interface is always accompanied by vapor diffusion. For the latter case with $C_{m,v\infty} = 1$, the vapor is directly condensed at the liquid–vapor interface without any mass diffusion. The different condensation mechanisms cause quite different heat and mass transfer ratios.

8. Conclusions

From this work, the following can be concluded.

1. This work is a successful investigation to apply the dimensionless velocity component method to the laminar free film condensation from vapor–gas mixture, for similarity analysis and transformation of whole system of the governing partial differential equations. The set of dimensionless variables of the transformed mathematical model greatly facilitates the analysis and calculation of the velocity, temperature and concentration fields, and heat and mass transfer of the film condensation from the vapor–gas mixture. It will be our successive work to apply the dimensionless velocity component method for extensive study on the related forced film condensation from the vapor–gas mixture.
2. In this work, three difficult points related to analysis and calculation of heat and mass transfer for the film condensation from the vapor–gas mixture have been well resolved. They include: (i) correct determination of the interfacial vapor condensate saturated temperature; (ii) reliable treatment of the concentration-dependent densities of vapor–gas mixture, and (iii) rigorously satisfying the whole set of physical matching conditions at the liquid–vapor interface. Meanwhile, the critical bulk vapor mass fraction for condensation was proposed, and evaluated for the film condensation from the water vapor–air mixture. Furthermore, advanced methods for treatment of temperature-dependent physical properties of liquids and gases were applied. On this basis, these analysis and calculation results are considered to be reliable.
3. The interfacial water vapor mass fraction $C_{v,ws}$ is exactly half of the bulk water vapor mass fraction $C_{v,w\infty}$, and only depends on $C_{v,w\infty}$ for the laminar free film condensation from the water vapor–air mixture.
4. The non-condensable gas has a decisive effect on the laminar free film condensation from vapor–gas mixture. Increasing the bulk gas mass fraction causes the condensate liquid film thickness, the condensate liquid velocity, and heat and mass transfer to decrease at an accelerated rate. Due to the different mechanisms with $C_{m,v\infty} \to 1$ and $C_{m,v\infty} = 1$, the heat and mass transfer is discontinuous at $C_{m,v\infty} = 1$ for the film condensation from the vapor–gas mixture.
5. Wall temperature is also a decisive variable in the condensate heat and mass transfer ratio. For a special bulk gas mass fraction, the increase of the wall temperature leads to the decrease of the wall sub-cooled temperature ratio $\frac{T_s - T_w}{(T_s)_{C_{m,v\infty}=1} - T_w}$, and, subsequently, leads to the decrease of the heat and mass transfer ratios of the film condensation from the vapor–gas mixture. In order to increase the efficiency of heat and mass transfer, the wall temperature should be as low as possible.

References

[1] D. Butterwoth, R.G. Sardesai, P. Griffith and A.E. Bergles, Condensation, in: Heat exchanger design handbook, Hemisphere, Washington, DC, Chapter 2.6, 1983.

[2] P.J. Marto, Fundamemtals of condensation, in: S. Kakac, A.E. Bergles, E.Q. Fernandes (Eds.), Two-phase flow heat exchangers: Thermal-hydraulic fundamentals and design, Kluwer Academic Publishers, Dordrecht, 1988, pp. 221–291.

[3] J.G. Collier, J.R. Thome, in: Convective Boiling and Condensation, third ed., Oxford University Press, Inc., New York, 1996, pp. 430–487.

[4] J.W. Rose, Condensation heat transfer, Heat Mass Transfer 35 (1999) 479–485.

[5] D.Y. Shang, Free convection film flows and heat transfer, Springer-Verlag, Berlin, Heidelberg and New York, 2006.

[6] W.J. Minkowycz, E.M. Sparrow, Condensation heat transfer in the presence of noncondensables, interfacial resistance, superheating, variable properties, and diffusion, Int. J. Heat Mass Transfer 9 (1966) 1125–1144.

[7] L. Slegers, R.A. Seban, Laminar film condensation of steam containing small concentration of air, Int. J. Heat Mass Transfer 13 (1970) 1941–1947.

[8] H.K. Al-Diwany, J.W. Rose, Free convection film condensation of steam in the presence of non-condensing gases, Int. J. Heat Mass Transfer 16 (1972) 1359–1369.

[9] R.K. Oran, C.J. Chen, Effect of lighter noncond-Nsa3l -Gas on laminar film condensation over a vertical plate, inc. J. Hear Mm Transfer. 18 (1975) 993–996.

[10] V.M. Borishanskiy, O.P. Volkov, Effect of uncondensable gases content on heat transfer in steam condensation in a vertical tube, Heat Transf.-Soviet Res. 9 (1977) 35–41.

[11] C.D. Morgan, C.G. Rush, Experimental measurements of condensation heat transfer with noncondensable gases present, in: 21st National Heat Transfer Conference, vol. 27, Seattle, Washington, ASME HTD, July 24–28, 1983.

[12] P.J. Vernier, P. Solignac, A test of some condensation models in the presence of a noncondensable gas against the ecotra experiment, Nucl. Technol. 77 (1) (1987) 82–91.

[13] S.M. Chiaasaan, B.K. Kamboj, S.I. Abdel-Khalik, Two-fluid modeling of condensation in the presence of noncondensables in two-phase channel flows, Nucl. Sci. Eng. 119 (1995) 1–17.

[14] H. Louahlia, P.K. Panday, Film condensation between two vertical flat plates - Comparison of the thermal performance of R134a and R12, Can. J. Chem. Eng. 75 (4) (1997) 704–711.
[15] Y.S. Chin, S.J. Ormiston, H.M. Soliman, A two-phase boundary-layer model for laminar mixed-convection condensation with a noncondensable gas on inclined plates, Heat Mass Transfer 34 (1998) 271–277.
[16] H.T. Chen, S.M. Chang, Z. Lan, Effect on noncondensable gas on laminar film condensation along a vertical plate fin, Int. J. Heat Fluid Flow 19 (4) (1998) 374–381.
[17] S.T. Revankar, D. Pollock, Laminar film condensation in a vertical tube in the presence of noncondensable gas, Appl. Math. Modell. 29 (4) (2005) 341–359.
[18] J.M. Martin-Valdepenas, M.A. Jimenez, F. Martin-Fuertes, J.A. Fernandez, Benitez, Comparison of film condensation models in presence of non-condensable gases implemented in a CFD Code, Heat Mass Transfer 41 (11) (2005) 961–976.
[19] S. Oh, S.T. Revankar, Experimental and theoretical investigation of film condensation with noncondensable gas, Int. J. Heat Mass Transfer 49 (15-16) (2006) 2523–2534.
[20] Y. Liao, K. Vierow, A generalized diffusion layer model for condensation of vapor with no-condensable gases, J. Heat Transfer 129 (8) (2007) 988–994.
[21] D.Y. Shang, T. Adamek, Study on laminar film condensation of saturated steam on a vertical flat plate for consideration of various physical factors including ariable thermophysical properties, Warme- und Stoffubertragung, vol. 30, Springer-Verlag, 1994, pp. 931–941.
[22] D.Y. Shang, B.X. Wang, An extended study on steady-state laminar film condensation of a superheated vapor on an isothermal vertical plate, Int. J. Heat Mass Transfer 40 (4) (1997) 931–941.
[23] VDI – Waermeatlas, Berechnungs Blaetter fuer Waemeubertragung, 5, erweiterte Auflage, VDI Verlag GmbH, Dusseldorf, (1988).